JHR 94: 247–269 (2022)
doi: 10.3897/jhr.94.91001
https://jhr.pensoft.net

RESEARCH ARTICLE

JOURNAL OF Hymenoptera RESEARCH
A peer-reviewed open-access journal
The International Society of Hymenopterists

Integrative approach resolves the taxonomy of *Eulaema cingulata* (Hymenoptera, Apidae), an important pollinator in the Neotropics

Tamires de Oliveira Andrade[1], Kelli dos Santos Ramos[1], Margarita M. López-Uribe[2], Michael G. Branstetter[3], Carlos Roberto F. Brandão[1]

1 *University of São Paulo, Museum of Zoology, Laboratory of Hymenoptera, São Paulo, Brazil* **2** *The Pennsylvania State University, Center for Pollinator Research, Department of Entomology, University Park, Pennsylvania 16802, USA* **3** *U.S. Department of Agriculture, Agricultural Research Service, Pollinating Insects Research Unit, Utah State University, Logan, Utah 84322, USA*

Corresponding author: Tamires de Oliveira Andrade (tamiresdeoliveirandrade@gmail.com)

Academic editor: Christopher K. Starr | Received 29 July 2022 | Accepted 26 October 2022 | Published 20 December 2022

https://zoobank.org/D2556958-A478-4508-8FEF-FF4B78FBB532

Citation: Andrade TO, Ramos KS, López-Uribe MM, Branstetter MG, Brandão CRF (2022) Integrative approach resolves the taxonomy of *Eulaema cingulata* (Hymenoptera, Apidae), an important pollinator in the Neotropics. Journal of Hymenoptera Research 94: 247–269. https://doi.org/10.3897/jhr.94.91001

Abstract

Species delimitation is a rich scientific field that often uses different sources of data to identify independently evolving lineages that might be recognized as species. Here, we use an integrative approach based on morphometrics, COI-barcoding, and phylogenomics using ultraconserved elements (UCEs) to investigate whether the orchid bee species *Eulaema cingulata* (Fabricius, 1804) and *E. pseudocingulata* Oliveira, 2006 represent a single variable taxon or two different species. We analyzed 126 specimens across the geographical range of these nominal species to test species hypotheses using the general lineage concept. We found substantial overlap in wing and head morphometrics, and both taxa form one phylogenetic lineage based on COI mitochondrial and UCE data. Our results support the recognition of both forms as members of the same evolutionary unit and *E. pseudocingulata* is herein recognized as a junior synonym of *E. cingulata*.

Keywords

DNA barcoding, morphometrics, orchid bees, phylogenomics, species delimitation, synonymy, ultraconserved elements

Introduction

Accurate species diagnosis remains a major challenge for many groups of organisms and is often described as the "taxonomic bottleneck" (Kim and Byrne 2006). On one hand, species identification can be challenging for evolutionary units that diverged recently because they may exhibit very similar morphology making them difficult to differentiate based on morphological traits alone. Difficulty in properly identifying cryptic species leads to underestimation of species diversity. On the other hand, conspecific individuals can display discrete polymorphism in morphological characters (e.g., Quezada-Euán et al. 2015; Lepeco and Gonçalves 2018) that, if used for taxonomic identification, may lead to the erroneous description of different species.

In order to circumvent some of the limitations of taxonomic classifications exclusively based on discrete qualitatively morphological characters, integrative taxonomy incorporates evidence from multiple independent datasets such as geometric morphometrics and molecular markers to inform species recognition and species boundaries (Goldstein and DeSalle 2010; Padial et al. 2010; Schlick-Steiner et al. 2010). Basing a species description on a variety of characters from different and independent datasets is generally regarded as the best practice (DeSalle et al. 2005). When species are considered as independently evolving lineages different lines of evidence are additive to each other (de Queiroz 2007).

Orchid bees (Hymenoptera: Apidae: Euglossini) are endemic to the Neotropical region. They receive their common name because males of these bees actively collect volatile compounds from orchids, and in the process pollinate the flowers (Dressler 1982). A variety of social behaviors are found among the euglossine genera, from solitary behavior to relatively complex social interactions in some species (Cameron 2004; Faria and Melo 2020). Five genera have been described in the tribe Euglossini: *Euglossa* Latreille, 1802, *Eufriesea* Cockerell, 1908, *Eulaema* Lepeletier, 1841, *Exaerete* Hoffmannsegg, 1817, and *Aglae* Lepeletier and Serville, 1825, encompassing approximately 240 species (Michener 2007; Moure et al. 2012). The genus *Eulaema* includes the largest orchid bees, with total body size varying from 18 to 30 mm in length (Oliveira 2000; Melo 2014), and is divided into two subgenera, *Apeulaema* and *Eulaema*, which are easily recognizable. Males of *Apeulaema* differ from *Eulaema* in having whitish-yellow spots on the clypeous, parocular areas and terga integument black, the latter sometimes turning to blue-violet (Moure 2000).

Eulaema (*Apeulaema*) *cingulata* (Fabricius, 1804) has a widespread distribution (from southern Brazil to southern Mexico), where it is associated mainly with wet and dry forested areas (Fig. 1A–C). This species is frequently sampled in faunistic inventories (e.g. Pires et al. 2013; Silveira et al. 2015; Machado et al. 2018) and reported in a wide range of ecological studies related to pollination in agroecosystems (Marques et al. 2017; Gutiérrez-Chacón et al. 2018), pollination of plants in Amazon rainforest (Martel et al. 2019; Watteyn et al. 2021), and as vectors of cleptoparasitic beetles (Rocha-Filho and Garófalo 2015).

Eulaema cingulata was initially described as *Centris cingulata* with no information on the number and sex of the specimens studied. The only information about these

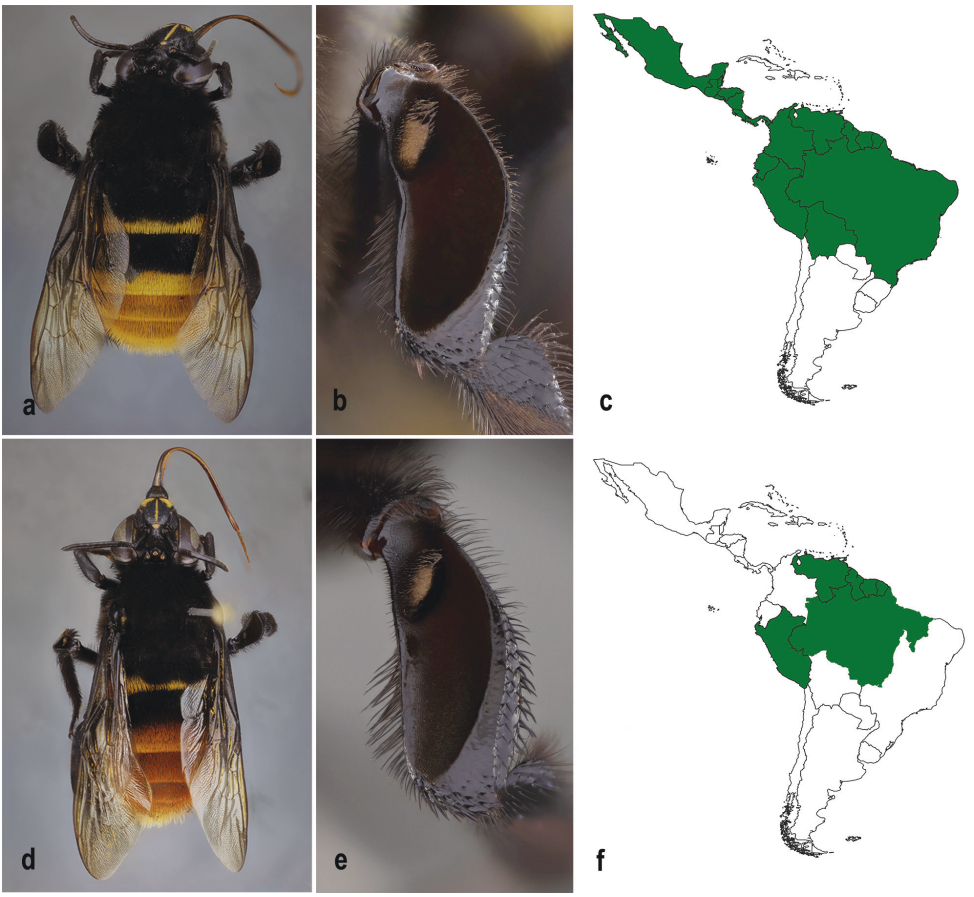

Figure 1. A, B male specimen of *Eulaema cingulata* from Sergipe, Brazil **A** body in dorsal view **B** velvety area in the mid tibia **C** geographical distribution of *E. cingulata* in green **D, E** male specimen of *E. pseudocingulata* from Pará, Brazil **D** body in dorsal view **E** velvety area in the mid tibia **F** geographical distribution of *E. pseudocingulata* in green.

specimens is their location as "*America meridionalis*" (according to Moure (1960) probably Guyana) and the institution in which they were deposited, the Zoologisk Museum in Copenhagen. In the species description, the first tergum and the base of the second are described as a single tergum, which led some authors to subsequent identification mistakes related to the color pattern of these terga. Lepeletier (1841), having specimens of *C. cingulata*, did not recognize them as such and described them as *E. fasciata*, based on a female, and *E. cajennensis*, based on a male (Moure 1960, 2000). Oliveira (2006) described *E.* (*Apeulaema*) *pseudocingulata* for specimens from the Amazon Forest (Fig. 1D–F) that show a morphologically distinct feature in the velvety area of the mid-leg of males. Males of *E. cingulata* have a wider posterior edge in the velvety area of the middle tibia than in *E. pseudocingulata* (Fig. 1B, E). In addition, the coloration of the male abdomen is darker in *E. pseudocingulata* than in *E. cingulata*.

Morphological differences between females of these two forms have not yet been found (Moure et al. 2012) and the female of *E. pseudocingulata* remains undescribed. Nemésio (2009) synonymized *E. pseudocingulata* under *E. cingulata* and proposed a new species (*E. marcii*) for the Atlantic Forest population, based on the misunderstood conclusion that this latter form had not been found in the type locality of *E. cingulata* (Melo in Moure et al. 2012). Moure et al. (2012) recently placed *Eulaema marcii* in synonymy with *E. cingulata* and adopted *E. pseudocingulata* as a taxonomically valid species as proposed by Oliveira (2006).

Despite the distinct differences in coloration and the velvety area of the mid-leg between males of *E. cingulata* and *E. pseudocingulata*, the taxonomic status of these nominal species has not been investigated with additional datasets. A comparative phylogeographic study of *E. cingulata* based on mitochondrial and nuclear markers revealed a lack of structure for *E. cingulata* throughout the whole range of the species (López-Uribe et al. 2014). That study included a small set of specimens from both *E. cingulata* and *E. pseudocingulata* and did not indicate genetic differentiation between these species. In the present study, we incorporate morphometric data (wings and heads) and molecular data from mitochondrial and genome-wide markers to test the status of both species. We used the character of the velvety area of the mid-leg of males for species identification of the specimens. Genetic and/or morphological clustering of specimens taxonomically identified based on this morphological character would support the presence of two evolutionary units.

Materials and methods

Morphometric data

We studied 107 specimens of *E. cingulata* and *E. pseudocingulata* from across their geographic ranges. Most of the specimens were collected in the Amazon forest where both species are sympatrically distributed (Fig. 2A, Suppl. material 1: table S1). Using a Leica DFC 295 camera, we photographed specimens attached to a stereomicroscope Leica M205C. For the analysis of wing morphometrics, we separated the right forewing from the body at the base of the radial vein using forceps and fixed it on glass microscopy slides. The heads were photographed in frontal view. For the image analysis, we saved photographs into TPS files using the software TpsUtil 1.60 (Rohlf 2013) and identified landmarks using the software tpsDig version 2.26 (Rohlf 2006). We selected 10 landmarks for the head (Fig. 3A), and 18 landmarks on the vein intersections for the wing (Fig. 3B). We choose the landmarks based on previous studies of bees (Quezada-Euán et al. 2015; Souza et al. 2015; Costa et al. 2020).

For comparisons of the overall wing and head sizes between species, we extracted the centroid size and used a generalized Procrustes analysis to capture shape variables without the effects of orientation and position of the images. A regression analysis between size and shape was performed to quantify the effect of allometry. Afterwards, we

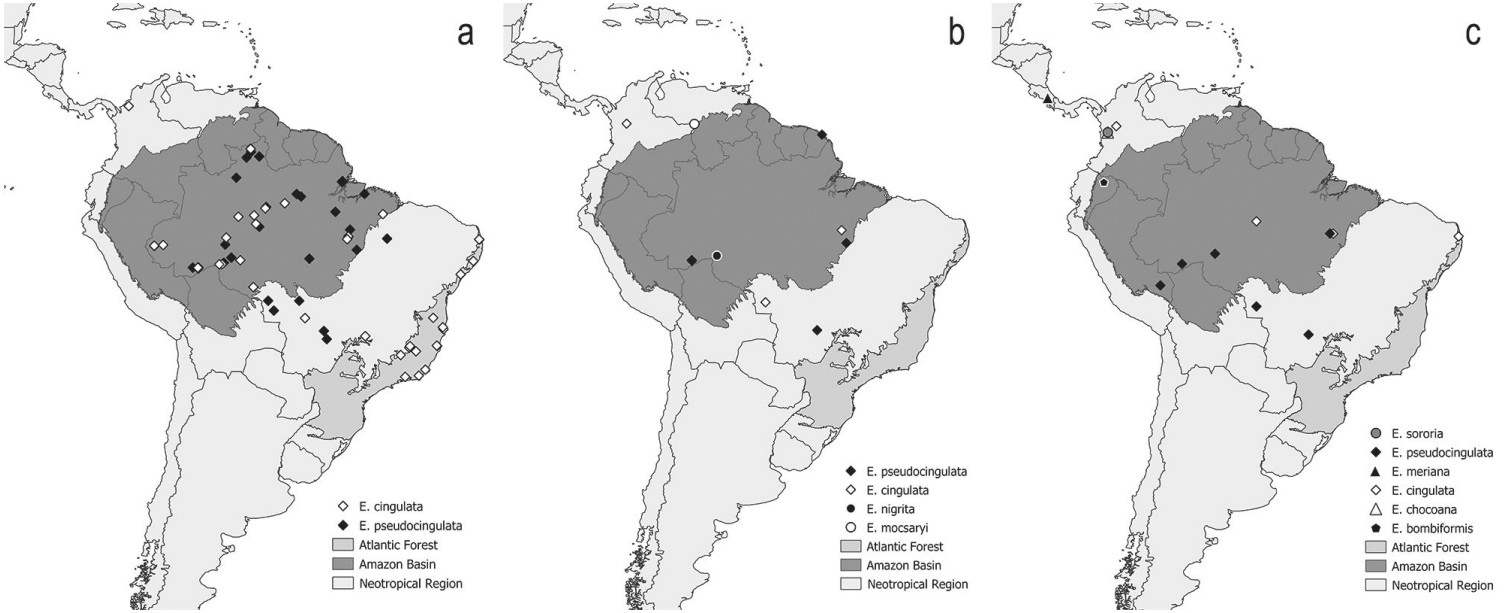

Figure 2. Geographical locality of the specimens used in each analysis of the present study **A** geometric morphometrics **B** COI-barcoding and pairwise genetic p-distance **C** phylogenomics using Ultraconserved elements.

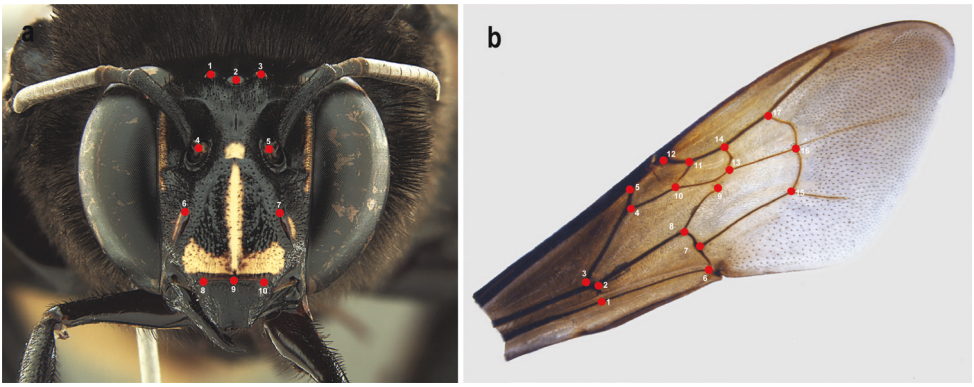

Figure 3. Landmarks used in the geometric morphometric analyses of *Eulaema cingulata* and *E. pseudocingulata* **A** head of male in frontal view and **B** forewing of male.

removed this allometric effect to independently quantify shape variation. The resulting landmark configurations retained only shape information (Klingenberg 2015).

To visually compare all individuals in multivariate trait space, we used a Principal Component Analysis (PCA) using the relative Cartesian coordinates of each landmark after alignment. The shape difference between species were tested using a Discriminant Analysis followed by a leave-one-out cross-validation test (Lachenbruch 1967). All analyses were performed using the software MorphoJ (Klingenberg 2011). Additionally, we used the percentages of correct classification to evaluate the discriminatory power of wing and head shapes.

DNA sampling, extraction, amplification, and sequencing

We extracted total genomic DNA from the hind legs or thoracic muscles of specimens using Qiagen DNeasy Kit (Qiagen) with modifications to maximize DNA yield for dry specimens as incorporated in Evangelista et al. (2012). Before extraction, we placed pinned specimens in a humid chamber for 24 hours to facilitate the removal of the leg or abdomen muscle without damaging the whole specimen. For tissue digestion, we added ATL buffer and 20µL of proteinase K (20 mg/ml) for the first six hours, and 10µL additionally after six hours of incubation at 55 °C .

We amplified sequences of the cytochrome oxidase I (COI) region using universal barcoding primers LCO (5'-GGTCAACAAATCATAAAGATATTGG-3') and HCO (5'-TAAACTTCAGGGTGACCAAAAAATCA-3') (Folmer et al. 1994). Polymerase Chain Reaction (PCR) amplifications were performed in a final volume of 17µl including 0.13 µL of Taq Polymerase (Qiagen) , 2µL of genomic DNA, 1.3µL of each primer (10µM), 3.4µL of dNTPs (10mM), 0.85µL of MgCl, 1.7µL of 10× Qiagen Buffer and 6.32µL of purified water. We performed amplification with an initial step of three minutes at 94 °C, followed by 40 cycles of 30 seconds at 94 °C, 30 seconds for annealing at 50 °C and 1 min at 72 °C. After 40 cycles, we performed a final step at 72 °C for 10 minutes. We performed all steps related to DNA extraction and COI

amplification at the Molecular Biology Laboratory of the Museu de Zoologia da Universidade de São Paulo, Brazil (MZSP). We sent the amplified COI fragments to Macrogen (Seoul, South Korea) for post-PCR purification and Sanger sequencing. We corroborated sequence quality by the quality scores provided by Macrogen and by visually examining the chromatograms using the software Ugene (Okonechnikov et al. 2012).

To include genome-wide markers in our dataset, we sequenced 2,180 Ultra Conserved Element (UCE) loci using a recently published bait set specific to bees, ants, and other apoid wasps ("hym-v2-bee-ant-specific"; Grab et al. 2019). This bait set is a subset of the principal Hymenoptera bait set first reported in Branstetter et al. (2017). For each sample, we sheared the DNA using a Qsonica Q800R2 acoustic sonicator, with the target fragment size range being 400-600 bp (60–120 secs shear time, 25% amplitude, 10–10 sec pulse). For older samples with more degraded DNA, we adjusted the shearing times to between 30-60 seconds. We cleaned fragmented DNA at 3× volume using a homemade SPRI-bead substitute ("speedbeads"; Rohland and Reich 2012). We generated Illumina sequencing libraries for each sample using Kapa Hyper Prep Kits (Roche Sequencing and Life Science, Wilmington, MA) and custom, dual-indexing adapters (Glenn et al. 2019).

We amplified libraries for 12 cycles, purified them using speedbeads (Rohland and Reich 2012), and quantified them using a Qubit 3.0 fluorometer (Thermo Fisher Scientific, Waltham, MA). To enrich UCE loci, we pooled 10 libraries at equimolar concentrations. Then, up to 500 ng of each pool was enriched following the manufacturer's protocol for day 1 (MYcroarray enrichment protocol v3.02) and the standard UCE protocol for day 2 (enrichment protocol v1.5 available at ultraconserved.org). The custom bait set was diluted 1:4 (1μL bait, 4μL H2O) with enrichment incubation at 65 °C for 24 hours using strip tubes and a PCR thermal cycler. For the second day of enrichment, we used 50uL of streptavidin beads per sample and performed on-bead PCR following the three heated (65 °C) wash steps. We amplified the enriched pools for 18 cycles and the resulting products were purified with SPRI beads at 1× volume. We sent the sequencing pools to the University of Utah Genomics Core for sequencing on an Illumina HiSeq 2500 (2×125, v4 chemistry).

Molecular approaches for species phylogeny and delimitation

For the molecular analyses, we generated DNA sequences from 19 males (less than 10 years old after collection) for the amplification of COI and UCEs. We preserved remaining body parts and associated DNA extractions for future studies (Suppl. material 1: table S2). Two sequences of the mitochondrial gene COI were obtained from GenBank and one sequence was obtained from BOLD Systems. We added the following other *Eulaema* species as outgroups: *E. meriana* (Olivier, 1789), *E. mocsaryi* (Friese, 1899) and *E. nigrita* Lepeletier, 1841 for COI analysis, and *E. bombiformis* (Packard, 1869), *E. chocoana* Ospina-Torres & Sandino-Franco, 1997, *E. meriana*, and *E. sororia* Dressler & Ospina-Torres, 1997 for the phylogenomic analysis (Suppl. material 1: table S2).

For the mitochondrial data, we aligned COI sequences using the multiple sequence alignment online tool MAFFT (Katoh et al. 2019) and manually edited them using

the software Ugene (Okonechnikov et al. 2012). We inferred a phylogenetic tree using Bayesian Inference (BI) method. Genetic distances within and between species were calculated in MEGA-X (Kumar et al. 2018) using 10,000 bootstraps. We performed Bayesian phylogenetic analyses in MrBayes v.3.2 (Ronquist et al. 2012) with COI sequences using the best nucleotide model estimated by PartitionFinder2 (Lanfear et al. 2017). The Markov Chain Monte Carlo (MCMC) was run for 20 million generations sampled every 1000th generation. We discarded 25 percent of the first trees as burnin. We visualized and edited the Bayesian trees in FigTree v. 1.4.4 (Rambaut 2018).

For the UCE dataset, we performed most data processing steps using the software package Phyluce (Faircloth 2016). We cleaned the reads for adapter contamination and low-quality bases using Illumiprocessor (Faircloth 2013), which functions as a wrapper around the software Trimmomatic (Bolger et al. 2014). We assembled cleaned reads *de novo* for each individual using SPAdes v. 3.12.0 (Bankevich et al. 2012). To identify UCE regions from the bulk of assembled contigs and to remove paralogs, we used the Phyluce script match_contigs_to_pobes and the HymV2-bee-ant UCE bait files from Grab et al. (2019). We aligned all the loci individually using MAFFT (Katoh and Standley 2013) as implemented in Phyluce package, and trimmed resulting alignments using Gblocks with reduced stringency parameters (Castresana 2000). We removed loci that had data for fewer than 75% of taxa and generated a concatenated matrix from the resulting alignment set.

For phylogenetic reconstruction using UCE data, we inferred phylogenetic trees using Maximum Likelihood (ML), and multi-species coalescence reconstruction . We performed maximum likelihood analyses using two different strategies: single concatenated alignment and partitioned based on the best-fitting partitioning scheme. For the concatenated alignment, we obtained the substitution model (TVM+F+R2) using ModelFinder (Kalyaanamoorthy et al. 2017) which is part of the IQ-TREE v2.1.1 software (Nguyen et al. 2015). The best-fitting partitioning scheme was obtained using Sliding-Window Site Characteristics (SWSC), which divides each UCE into three data blocks corresponding to the right flank, core, and left flank (Tagliacollo and Lanfear 2018). We analyzed the resulting data subsets using PartitionFinder2 (Lanfear et al. 2017) using the rclusterf algorithm with AICc model selection criterion and GTR+G model of sequence evolution obtained by ModelFinder. We used the likelihood-based program IQ-Tree v2.1.1 for phylogenetic reconstruction of both partitioning schemes. To assess branch support, we performed 1000 replicates of the ultrafast bootstrap approximation (UFBoot; Hoang et al. 2018) and 1000 replicates of the branch-based Shimodaira-Hasegawa approximate likelihood-rate test (SH-aLRT; Guindon et al. 2010) using the command '-alrt'. Only clades with support values of UFBoot ≥ 0.95 and SH-aLRT ≥ 0.80 were considered robust. To account for heterogeneous gene histories that may influence phylogenetic accurate resolution, we inferred a species tree under the multi-species coalescent model using the program ASTRAL-III v.5.7.3 (Zhang et al. 2018), using gene trees provided by IQ-Tree as input. Support was assessed as local posterior probability, with ≥ 0.95 considered robust.

We also estimated a coalescent-based species tree using *Beast (Heled and Drummond 2010) and the BEAST2 package (Bouckert et al. 2019). Due to computational constraints, we selected a subset of loci for the *BEAST analysis. We ran the command

'phyluce_align_get_informative_sites' from Phyluce to identify the 100 most informative genes. From these most informative genes, we then selected those that were present in all samples, resulting in 88 UCEs. The analysis was run for 100 million generations sampling every 10,000 generations under a strict clock model with a constant population model, and a Yule model as a tree prior. We used a GTR model (unlinked across loci) for the nucleotide substitution model that was provided by PartitionFinder2 (Lanfear et al. 2017). To examine the convergence across the four runs performed and the ESS values of sampled parameters, we used Tracer v1.7 (Rambaut et al. 2018). A maximum clade credibility was constructed in TreeAnnotator and visualized the tree using Densitree, both included in the BEAST package (Bouckert et al. 2019).

Data availability

The raw UCE sequence reads have been uploaded to the NCBI Sequence Read Archive under BioProject accession PRJNA875942.

Results

Morphometric geometrics

Individuals identified as *E. cingulata* and *E. pseudocingulata* formed one cluster based on the shape of the head and wings (Fig. 4). The PCA captured the variation of head and wing shape in 8 and 32 PCs, respectively. The first three components of the head variation explained 45.28%, 19.16%, and 12.37% of the covariance, respectively, total ing 76.81% (Suppl. material 1: table S3). The cross-validation test correctly located

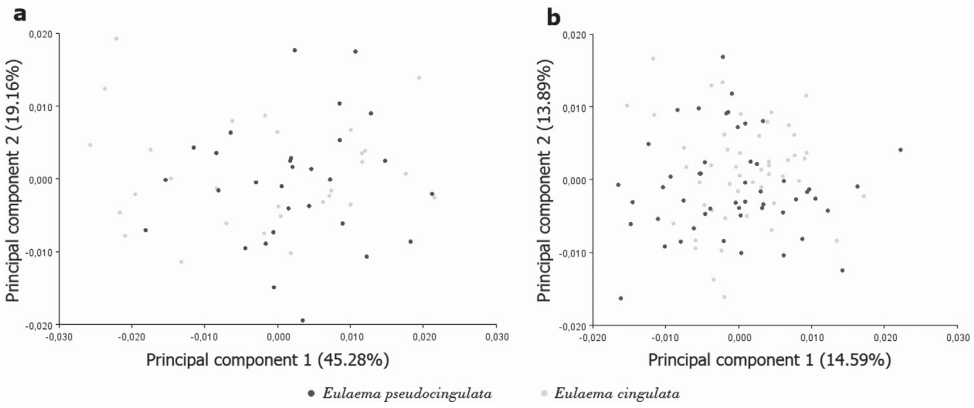

Figure 4. Shape variation of males of *Eulaema* species grouped considering **A** the shape of the head, and **B** the shape of the wings: The percentage explained by each Principal Components (PC) is in parenthesis. The negative and positive extremes of both PC1 and PC2 are shown below and besides of the graph (Factor scale: left -0.03, right 0.03).

Table 1. Cross-validated classification rates of correct group assignments between male specimens of *Eulaema cingulata* and *Eulaema pseudocingulata* based on head and wing shapes.

	Head			
	E. cingulata	***E. pseudocingulata***	**Total**	**%**
E. cingulata	18	11	29	62.07
E. pseudocingulata	10	20	30	66.67
		Wing		
E. cingulata	33	17	50	66
E. pseudocingulata	16	34	50	68

62.07% and 66.67% of specimens of *E. cingulata* and *E. pseudocingulata*, respectively. The first three components of the wing shape explained 13.32%, 10.84%, and 10.02% of the variance, respectively, explaining a total of 34.18% of the variation (Suppl. material 1: table S4). Similar to the head results, the cross-validation test correctly located 66% and 68% of specimens of *E. cingulata* and *E. pseudocingulata*, respectively (Table 1). The multivariate regression analysis showed that, after 10,000 permutation rounds, the influence of the allometric effect was statically significant ($P < 0.0001$) with 32.28% and 3.07% predicted shape variation of the head and wing shape, respectively. Nonetheless, even after removing this allometric effect, the groups remained undifferentiated.

Genetic distance

The 655 bp fragment of the mitochondrial COI region resulted in an average pairwise genetic p-distance within *E. cingulata* of 1.3% and within *E. pseudocingulata* of 0.7%, while between the two species was 0.9%. The greater amount of genetic differentiation within the group of *E. cingulata* than between specimens from the two nominal species indicated no support for the presence of two evolutionarily independent units. The average pairwise genetic distances among *E. cingulata* and the outgroups (*Eulaema mocsaryi*, *E. nigrita*, and *E. meriana*) are greater than 5.6% (Table 2).

Table 2. Average pairwise genetic p-distance between species of *Eulaema* employing COI sequences with 655pb aligned.

Species	***Eulaema cingulata***	***Eulaema pseudocingulata***
Eulaema cingulata	1.3%*	0.9%
Eulaema pseudocingulata	0.9%	0.7%*
Eulaema mocsaryi	5.6%	5.3%
Eulaema nigrita	9.3%	9.0%
Eulaema meriana	11.2%	11.3%

*Average pairwise genetic p-distance within each species.

Phylogenetic relationships

Both the COI and UCE phylogenetic reconstructions provided no support for the species differentiation of *E. cingulata* and *E. pseudocingulata* (Figs 5, 6). For COI, PartitionFinder2 identified GTR+I as the best nucleotide substitution mod-

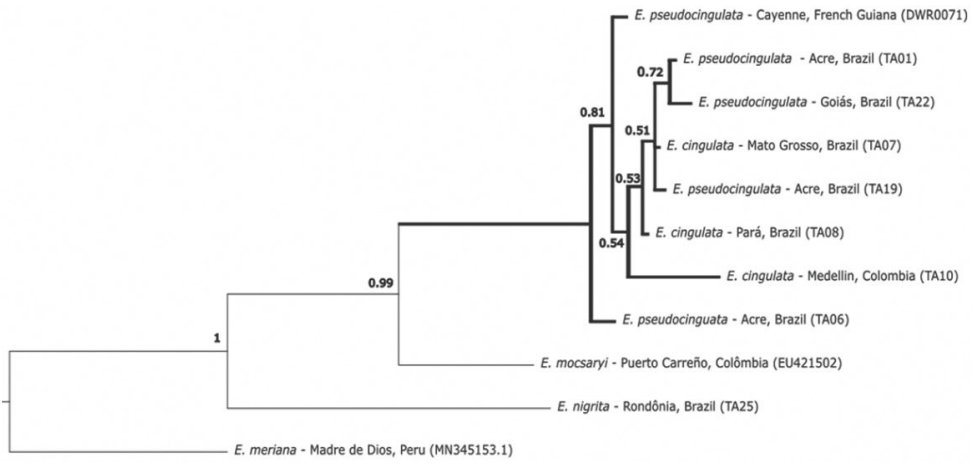

Figure 5. Consensus tree for *Eulaema cingulata* and *E. pseudocingulata* resulting from a Bayesian analysis of molecular data from the gene COI. Numbers on branches indicate posterior probability support . Geographical location of each individual is shown in each tip.

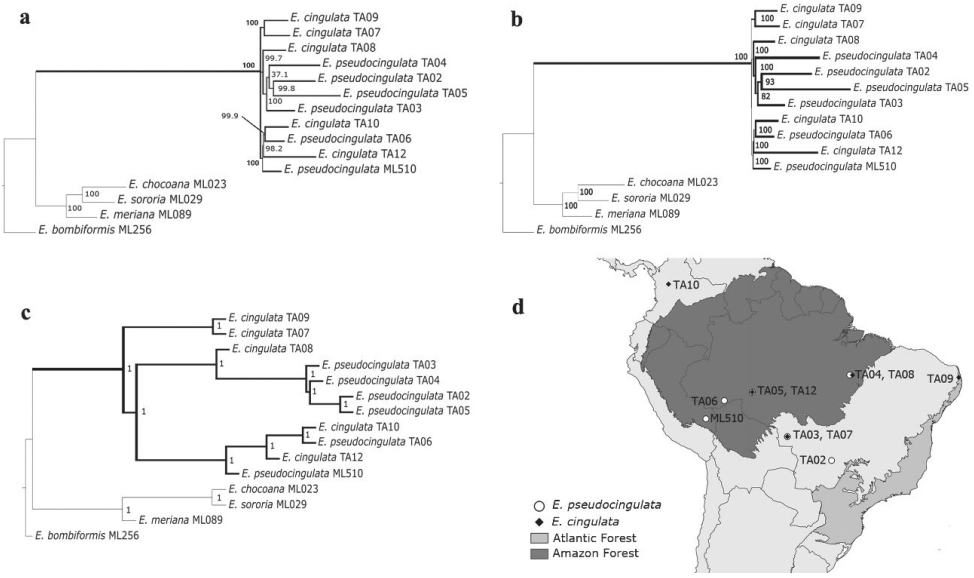

Figure 6. Phylogenetic trees for *Eulaema cingulata* and *E. pseudocingulata* obtained with Ultraconserved Elements (UCE) **A** maximum likelihood phylogenetic tree obtained with concatenated dataset in IQ -Tree. Numbers on nodes correspond to ultrafast bootstrap **B** maximum likelihood phylogenetic tree obtained with partitioned dataset in IQ -Tree. Numbers on nodes correspond to ultrafast bootstrap **C** species delimitation analyses based on multispecies-coalescent model obtained with ASTRAL. Number on nodes corresponds to posterior probabilities **D** map showing the distribution of the analyzed material (ingroup).

el. The consensus tree obtained from MrBayes showed that the COI fragments grouped *E. cingulata* and *E. pseudocingulata* into one highly supported clade sister to *E. mocsaryi* (Fig. 5). For the UCE data, we recovered a total of 21,470,135 reads

with an average of 1,431,342 reads per sample (range = 513,594 – 2,585,935). These reads were assembled into an average of 186,700 contigs per sample (range = 34,358 – 441,504), having an average length of 167bp. An average (per sample) of 2,217 of contigs match UCE loci from the target capture probes used. Following alignment, trimming, and filtering of the UCE loci, our final UCE matrix consisted of 2,180 loci and 1,509,760 bp of sequence data, of which 33,722 bp are informative. The average length of UCE contigs post alignment and trimming is about 692 bp (range = 229 – 1,831).

The maximum likelihood inference of the UCEs markers recovered identical topologies from both partitioned and concatenated schemes, with most nodes showing high support (Fig. 6A, B). Individuals identified as *E. cingulata* and *E. pseudocingulata* form a monophyletic group with maximum support value. The difference between these topologies is limited to the phylogenetic position of *E. pseudocingulata* TA03 and TA04 within a small *pseudocingulata* clade. The only individual from the Atlantic Forest (*E. cingulata* TA09) is recovered with maximum support as sister to the individual from Mato Grosso (*E. cingulata* TA07), a state in the Amazon Forest. The ASTRAL and * Beast species tree showed maximum support values and both recovered the same topology (illustrated by the ASTRAL tree on Fig. 6C). Even though the COI and UCE data included different samples, both methods present very similar topologies with no significant differences between the individuals grouped in the two nominal species. Both trees showed one clade with individuals from the two species with high statistical support.

Discussion

Our results indicate that specimens identified as *E. cingulata* and *E. pseudocingulata* do not show morphological or genetic differentiation. Geometric morphometrics of the forewings has been previously used as a powerful technique to discriminate bee species (Francoy et al. 2012; Combey et al. 2013), subspecies (Oleksa and Tofilski 2014; Silva et al. 2015), cryptic species (Francisco et al. 2008; Hurtado-Burillo et al. 2016) and geographical ecotypes (Francoy et al. 2011; Grassi-Sella et al. 2018; Carneiro et al. 2019). Using both landmarks and outlined-based methodologies, Francoy et al. (2012) showed that the use of this approach to discriminate *Euglossa* species was more effective than studies using allozymes and restriction patterns of mitochondrial genes. Quezada-Euán et al. (2015) identified differences in wing shape of the two different morphs of *Euglossa viridissima* Friese, 1899 that had been only otherwise identified by the number of mandibular teeth. We applied the same methodology to this study to assess the taxonomic status of the two focal species in the genus *Eulaema*. Similarly, the results obtained with the head measurements were congruent with the results obtained with the forewings. Despite being used less frequently than the wings, the use of landmarks on the head has also been informative to recognize intercastes in honey bees (Souza et al. 2015), and to discriminate the morphologically indistinguishable females of the *Psychodopygus* complex (Diptera) (Godoy et al. 2018).

Because the level of morphological differentiation among recently divergent lineages is sometimes insufficient to recognize species, we used mitochondrial and UCE data to test the presence of genetically distinct groups of individuals among the specimens studied. DNA barcodes are increasingly becoming a standard tool used by taxonomists and its association with morphological characters has proven useful at discriminating species in several groups of bees (Gibbs 2009). Although this method has been criticized by some authors (Rubinoff et al. 2006; Wheeler 2008), it gives additional support to the recognition of species when considered along with other data sources (Padial and De La Riva 2007; Packer et al. 2009). Based on our data, the pair wise sequence divergences within and between the two species were below 3%, which according to Hebert et al. (2003) is a result compatible with the expected variation within a single species. More importantly, specimens of *E. cingulata* and *E. pseudocingulata* did not form a distinct monophyletic clades and the genetic distance among individuals of *E. cingulata* was greater than the genetic distance among individuals of *E. cingulata* and *E. pseudocingulata*. Dick et al. (2004) found that mtDNA divergences within Euglossini species were consistently low, with divergences among populations separated by the Andes averaging 1.1% (collection sites cover 3,000km). These findings and other studies have indicated the presence of high levels of long-distance gene flow between orchid bee populations. Rocha-Filho et al. (2013) observed a comparatively high dispersal ability in *E. cingulata* through genetic analyses comparing mainland and island populations. López-Uribe et al. (2014) also found low values of mitochondrial nucleotide divergence between populations of three species of *Eulaema*, showing a minimum value of 0.39% within species divergence in *E. cingulata*. According to the authors, the low sequence divergence between populations of *E. cingulata* was partially explained by the recent origin of this species.

The topology obtained with genomic data also supports the monophyly and recognition of one clade that comprises *E. cingulata* and *E. pseudocingulata*. UCEs have been successfully used as a tool for species discrimination as they provide sufficient variation at shallow time scales (Smith et al. 2013; Gueuning et al. 2020). Combined phylogenetic and population genetic approaches have been effectively used to investigate boundaries between complexes of wild European bees suspected to harbor cryptic diversity, mitochondrial introgression, or mitochondrial paraphyly (Gueuning et al. 2020). Using COI and UCEs with the multispecies coalescent method (BPP), Gueuning et al. (2020) also concluded that UCEs can provide robust species hypotheses and outperform COI in species delimitation. The adoption of delimitation methods based on the multispecies coalescent model has been criticized by Sukumaran and Knowles (2017), who argued that these methods tend to delimit population structure instead of species. The authors' concern was raised by the possibility of taxonomic inflation if species are described based only on molecular data. However, most studies using genetic data in species delimitation also incorporate addiotal sources of data such as morphology or morphometrics.

Herein, we conclude that *E. pseudocingulata* is not an independent evolutionary lineage from *E. cingulata* suggesting that the morphological differences observed in the

Figure 7. Color of the pilosity on the metasoma of males from Amazon Forest **A** *Eulaema cingulata* (Brazil, Pará, Cachimbó) **B** *Eulaema cingulata* (Brazil, Pará) **C** *Eulaema pseudocingulata* (Brazil, Pará, Canaã dos Carajás) **D** *Eulaema pseudocingulata* (Brazil, Acre, Rio Branco).

velvety area of the mid-leg of males are a species polymorphism in *E. cingulata*. The difference in the shape of the mid tibia velvety area, proposed as the diagnostic character between the species, can be interpreted as a variable condition: it can be narrower and farther from the rear edge in some morphs occurring in the Amazon forest, or wider and closer to the rear edge in morphs occurring throughout the species distribution. Initially, the color of the abdomen was also proposed as a diagnostic character to differentiate *E. cingulata* and *E. pseudocingulata*, but a gradient can be observed in the two morphs, varying from a yellowish tone to orange (Fig. 7A–D). Additionally, color can be a highly variable trait within bees making it a difficult character for taxonomic identification. Variable color patterns on the abdomen have been described for several species of bumble bees (e.g., Carolan et al. 2012; Huang et al. 2015). Color variation in Eucerini bees was reported by Grando et al. (2018), in which they found two distinct color patterns in sympatric populations of *Melissodes nigroaenea* (Smith, 1854) in Brazil. Variation in color and shape was observed in *Augochlora amphitrite* (Schtottky, 1909) by Lepeco and Gonçalves (2018) using morphometric analyses and studying the male genital capsules. The authors did not find any character that support the recognition of distinct color morphs and macrocephalic females as different species. Similar to our findings, a genetic study of different color morphs of *Euglossa* species from the Atlantic Forest did not support the recognition of different species (Ferrari and Melo 2014).

The mechanisms responsible for maintaining the variation of the velvety area of the mid tibia in individuals of *E. cingulata* in the Amazon Forest remain unknown. However, a plausible explanation for the lack of differentiation in morphological and genetic markers is that there is an ongoing speciation process driven by sexual selection in the Amazonian population of *E. cingulata*. Such a rapid speciation process has been described in two sympatric *Euglossa* species from southern Mexico: *E. viridissima* and *E. dilemma* (Eltz et al. 2011). These sister species can be partially differentiated by the number of mandibular teeth: *E. dilemma* males possess three teeth on the mandibles while *E. viridissima* mostly show two teeth with some individuals expressing three teeth. However, these species are unequivocally distinguished by chemical characters (cuticular hydrocarbons found in the hind tibia) as well as by highly variable DNA markers (microsatellites and SNPs) (Pokorny et al. 2014; Quezada-Euán et al. 2015).

A similar process could be occurring in *E. cingulata* and *E. pseudocingulata* but chemical information and characterization of genetic polymorphism across the entire genome of these bees would be necessary to properly investigate these questions. Further investigations are necessary to understand potential processes of incipient speciation in characters that have been characterized thus far.

Taxonomy

Eulaema (*Apeulaema*) *cingulata* (Fabricius 1804)

Centris cingulata Fabricius 1804: 355. Lectotype female, *'America meridionalis'* (probably Guyana according to Moure 1960).
Eulaema cajennensis Lepeletier 1841: 14. Lectotype male, French Guiana, Cayenne.
Eulaema fasciata Lepeletier 1841: 12. Lectotype female, French Guiana, Cayenne.
Eulaema (*Apeulaema*) *marcii* Nemésio 2009: 175. Holotype male, Brazil, Minas Gerais.
Eulaema (*Apeulaema*) *pseudocingulata* Oliveira 2006: 122. Holotype male, Brazil: Amazonas. New synonymy.

Diagnosis and comments. We recognized the taxon present in the Amazon forest under the name *E. pseudocingulata* as a junior synonym of *E. cingulata*, in light of the morphometric and phylogenetic data presented here. *E. cingulata* includes individuals with velvety areas of the midtibia that vary in width of the smooth area near the posterior edge (Fig. 1B, E). The basal tuft can be narrower or wider and slightly sloping. Other characters in this species include the labrum with lateral carina smoothly curved at the apex and ending distantly the edge of the clypeus, and the middle carina much shorter than lateral carina. The color of the metasomal hairs varies from orange to a light yellowish color (Fig. 7A–D). The material examined is the same as referenced in the Suppl. material 1: tables S1, S2. Lectotype of *Eulaema cingulata* was examined by the images available in Nemésio (2009) and the holotype of *E. pseudocingulata* in Almeida et al. (2020).

Conclusion

We tested the species hypothesis of *Eulaema cingulata* and *E. pseudocingulata* by integrating multiple independent datasets: geometric morphometrics, phylogenetics using mitochondrial DNA, and phylogenomics using ultraconserved elements. All results across methods were congruent, showing no separation between morphs previously recognized as different species. Our results also suggest that the morphology of the mid tibia of *E. pseudocingulata*, proposed as the diagnostic character between the morphs, appears as a variable condition in some individuals of *E. cingulata* from the Amazon basin. Besides the variation in the mid leg, there is also color variation across samples. The evolutionary drivers of this variability are currently unknown. In the interests of nomenclatural stability, we have designated *E. pseudocingulata* as a junior synonym of

E. cingulata. Orchid bees are important pollinators in Neotropical forests, being widely used in environmental quality studies, and they have become a good model for evolutionary genetics studies. However, as shown here, there is still a need to improve knowledge of the alpha taxonomy of these important group of Neotropical pollinators. Integration of DNA sequence analyses with geometric morphometrics of heads and wings can more rigorously test species boundaries than traditional morphological assessments alone and can ultimately improve species descriptions and identification tools.

Acknowledgements

We thank the curators and technicians of the collections for the loan of bee specimens: Elder Morato (Universidade Federal do Acre), Beatriz Coelho and Orlando Silveira (Museu Paraense Emílio Goeldi), Márcio Oliveira (Instituto Nacional de Pesquisas da Amazônia), Fernando Silveira and José Eustáquio (Universidade Federal de Minas Gerais), Maria Cristina Gaglianone (Universidade Estadual do Norte Fluminense Darcy Ribeiro). We thank José Villavicencio (Museu de Zoologia da Universidade de São Paulo - MZSP) for the support with the morphometric analyses, and Nathaniel Pope (Pennsylvania State University), Sergio Bolivar and Luz Eneida (MZSP) for the assistance with genomic data. This work was supported by Coordenação de Aperfeiçoamento de Pessoal de Nível Superior (Capes), funding code 001 (TOA), Fundação de Amparo à Pesquisa do Estado de São Paulo (Fapesp), process 17/07366-1 and 2016/50378-8 (CRFB and TOA). MML-U was funded through the USDA NIFA Appropriations under Projects PEN04716 and PEN04620. MGB and part of the sequencing work was funded through USDA project 2080-21000-019-000-D and NSF grant DEB-2127744. USDA is an equal opportunity provider and employer.

References

Almeida EAB, Costa AM, Filho JAT, Zichinelli MMP, Quinteiro FB (2020) Illustrated catalogue of type specimens of insects (Hexapoda) at Coleção Entomológica "Prof. J.M.F. Camargo" (RPSP), Universidade de São Paulo, Brazil. Zootaxa 4842(1): 1–204. https://doi.org/10.11646/zootaxa.4842.1.1

Bankevich A, Nurk S, Antipov D, Gurevich AA, Dvorkin M, Kulikov AS, Lesin VM, Nikolenko SI, Pham S, Prjibelski AD, Pyshkin AV, Sirotkin AV, Vyahhi N, Tesler G, Alekseyev MA, Pevzner PA (2012) SPAdes: a new genome assembly algorithm and its applications to single-cell sequencing. Journal of Computational Biology 19: 455–477 https://doi.org/10.1089/cmb.2012.0021

Bolger AM, Lohse M, Usadel B (2014) Trimmomatic: a flexible trimmer for Illumina sequence data. Bioinformatics 30: 2114–2120. https://doi.org/10.1093/bioinformatics/btu170

Bouckaert RR, Vaughan TG, Barido-Sottani J, Duchene S, Fourment M, Gavryushina A, Heled J, Jones G, Kühnert D, Maio N, Matschiner M, Mendes FK, Müller NF, Ogilvie HA, Plessis L, Popinga A, Rambaut A, Rasmussen D, Siveroni I, Suchard MA, Wu C-H, Xie D, Zhang C, Stadler T, Drummond AJ (2019) BEAST 2.5: An advanced software

platform for Bayesian evolutionary analysis. PLoS Computational Biology 15: e1006650. https://doi.org/10.1371/journal.pcbi.1006650

Branstetter MG, Longino JT, Ward PS, Faircloth BC (2017) Enriching the ant tree of life: enhanced UCE bait set for genome-scale phylogenetics of ants and other Hymenoptera. Methods in Ecology and Evolution 8: 768–776. https://doi.org/10.1111/2041-210x.12742

Cameron SA (2004) Phylogeny and biology of neotropical orchid bees (Euglossini). Annual Review of Entomology 49: 377–404. https://doi.org/10.1146/annurev.ento.49.072103.115855

Carneiro LS, Aguiar CML, Aguiar WM, Aniceto ES, Nunes LA, Ferreira VS (2019) Morphometric variability among populations of *Euglossa cordata* (Hymenoptera: Apidae: Euglossini) from different phytophysiognomies. Sociobiology 66(4): 575–581. https://doi.org/10.13102/sociobiology.v66i4.4675

Carolan JC, Murray TE, Fitzpatrick Ú, Crossley J, Schmidt H, Cederberg B, McNally L, Paxton RJ, Williams PH, Brown MJF (2012) Color patterns do not diagnose species: quantitative evaluation of a DNA barcode cryptic bumblebee complex. PLoS ONE 7: e29251. https://doi.org/10.1371/journal.pone.0029251

Castresana J (2000) Selection of conserved blocks from multiple alignments for their use in phylogenetic analysis. Molecular Biology and Evolution 17: 540–552. https://doi.org/10.1093/oxfordjournals.molbev.a026334

Combey R, Teixeira JSG, Bonatti V, Kapwong P, Francoy TM (2013) Geometric morphometrics reveals morphological differentiation within four African stingless bee species. Annals of Biological Research 4: 95–105.

Costa CP, Machado CAS, Santiago WMS, Dallacqua RP, Garófalo CA, Francoy TM (2020) Biome variation, not distance between populations, explains morphological variability in the orchid bee *Eulaema nigrita* (Hymenoptera, Apidae, Euglossini). Apidologie 51: 984–996. https://doi.org/10.1007/s13592-020-00776-z

DeSalle R, Egan MG, Siddall M (2005) The unholy trinity: taxonomy, species delimitation and DNA barcoding. Philosophical Transactions of the Royal Society B 360: 1905–1916. https://doi.org/10.1098/rstb.2005.1722

De Queiroz K (2007) Species concepts and species delimitation. Systematic Biology 56: 879–886. https://doi.org/10.1080/10635150701701083

Dick CW, Roubik DW, Gruber KF, Bermingham E (2004) Long-distance gene flow and cross-Andean dispersal of lowland rainforest bees (Apidae: Euglossini) revealed by comparative mitochondrial DNA phylogeography. Molecular Ecology 13: 3775–3785. https://doi.org/10.1111/j.1365-294X-2004.02374.x

Eltz T, Fritzsch F, Pech JR, Zimmermann Y, Ramírez SR, Quezada-Euán JJG, Bembé B (2011) Characterization of the orchid bee *Euglossa viridissima* (Apidae: Euglossini) and a novel cryptic sibling species, by morphological, chemical, and genetic characters. Zoological Journal of the Linnean Society 163: 1064–1076. https://doi.org/10.1111/j.1096-3642.2011.00740.x

Evangelista O, Sakakibara AM, Cryan JR, Urban JM (2012) A phylogeny of the treehopper subfamily Heteronotinae reveals convergent pronotal traits (Hemiptera: Auchenorrhyncha: Membracidae). Systematic Entomology 42: 410–428. https://doi.org/10.1111/syen.12221

Faircloth BC (2013) Illumiprocessor: a trimmomatic wrapper for parallel adapter and quality trimming. https://doi.org/10.6079/J9ILL

Faircloth BC (2016) PHYLUCE is a software package for the analysis of conserved genomic loci. Bioinformatics 32: 786–788. https://doi.org/10.1093/bioinformatics/btv646

Faria LRR, Melo GAR (2020) Orchid bees (Euglossini). In: Starr C (Ed.) Encyclopedia of Social Insects. Springer, Cham, 1–6. https://doi.org/10.1007/978-3-319-90306-4_91-1

Ferrari BR, Melo GAR (2014) Deceiving colors: recognition of color morphs as separate species in orchid bees is not supported by molecular evidence. Apidologie 45: 641–652. https://doi.org/10.1007/s13592-014-0280-7

Folmer O, Black M, Hoeh W, Lutz R, Vrijenhoek R (1994) DNA primers for amplification of mitochondrial cytochrome c oxidase subunit I from diverse metazoan invertebrates. Molecular Marine Biology and Biotechnology 3: 294–299.

Francisco FO, Nunes-Silva P, Francoy TM, Wittmann D, Imperatriz-Fonseca VL, Arias MC, Morgan ED (2008) Morphometrical, biochemical and molecular tools for assessing biodiversity. An example in *Plebeia remota* (Holmberg, 1903) (Apidae, Meliponini). Insectes Sociaux 55: 231–237. https://doi.org/10.1007/s0004-008-0992-7

Francoy TM, de Faria Franco F, Roubik DW (2012) Integrated landmark and outline-based morphometric methods efficiently distinguish species of *Euglossa* (Hymenoptera, Apidae, Euglossini). Apidologie 43: 609–617. https://doi.org/10.1007/s13592-012-0132-2

Francoy TM, Grassi ML, Imperatriz-Fonseca VL, May-Itzá WJ, Quezada-Euán JJG (2011) Geometric morphometrics of the wing as a tool for assigning genetic lineages and geographic origin to *Melipona beecheii* (Hymenoptera: Meliponini). Apidologie 42: 499–507. https://doi.org/10.1007/s13592-011-0013-0

Gibbs J (2009) Integrative taxonomy identifies new (and old) species in the *Lasioglossum* (*Dialictus*) *tegulare* (Robertson) species group (Hymenoptera, Halictidae). Zootaxa 2032: 1–38. https://doi.org/10.11646/zootaxa.2032.1.1

Glenn TC, Pierson TW, Bayona-Vásquez NJ, Kieran TJ, Hoffberg SL, Thomas IVJC, Lefever DE, Finger JJW, Gao B, Bian X, Louha S, Kolli RT, Bentley K, Rushmore J, Wong K, Shaw TI, Rothrock JMJ, McKee AM, Guo TL, Mauricio R, Molina M, Cummings BS, Lash LH, Lu K, Gilbert GS, Hubbell SP, Faircloth BC (2019) Adapterama II: universal amplicon sequencing on Illumina platforms (TaggiMatrix). PeerJ 7: e7786. https://doi.org/10.7717/peerj.7786

Godoy RE, Shimabukuro PHF, Santos TV, Pessoa FAC, Cunha AEFL, Santos FKM, Vilela ML, Rangel EF, Galati EAB (2018) Geometric morphometry of the head in sand flies (Diptera: Psychodidae: Phlebotominae), an alternative approach to taxonomy studies. Zootaxa 4504: 566–576. https://doi.org/10.11646/zootaxa.4504.4.7

Goldstein PZ, DeSalle R (2010) Integrating DNA barcode data and taxonomic practice: determination, discovery, and description. Bioessays 33: 135–147. https://doi.org/10.1002/bies.201000036

Grab H, Branstetter MG, Amon N, Urban-Mead KR, Park MG, Gibbs J, Blitzer EJ, Poveda K, Loeb G, Danforth BN (2019) Agriculturally dominated landscapes reduce bee phylogenetic diversity and pollination services. Science 363: 282–284. https://doi.org/10.1126/Science.aat6016

Grando C, Amon ND, Clough SJ, Guo N, Wei W, Azevedo P, López-Uribe MM, Zucchi MI (2018) Two colors, one species: the case of *Melissodes nigroaenea* (Apidae: Eucerini), an important pollinator of cotton fields in Brazil. Sociobiology 65: 645–653. https://doi.org/10.13102/sociobiology.v65i4.3464

Grassi-Sella ML, Garófalo CA, Francoy TM (2018) Morphological similarity of widely separated populations of two Euglossini (Hymenoptera; Apidae) species based on geometric morphometrics wings. Apidologie 49: 151–161. https://doi.org/10.1007/s13592-017-0536-0

Gueuning M, Frey JE, Praz C (2020) Ultraconserved yet informative for species delimitation: UCEs resolve long-standing systematic enigma in Central European bees. Molecular Ecology 29: 4203–4220. https://doi.org/10.1111/mec.15629

Guindon S, Dufayard JF, Lefort V, Anisimova M, Hordijk W, Gascuel O (2010) New algorithms and methods to estimate maximum likelihood phylogenies: assessing the performance of phyml 3.0. Systematic Biology 59: 307–321. https://doi.org/10.1093/sysbio/syq010

Gutiérrez-Chacón C, Fornoff F, Ospina-Torres R, Klein A-M (2018) Pollination of Granadilla (*Passiflora ligularis*) benefits from large wild insects. Journal of Economic Entomology 111: 1526–1534. https://doi.org/10.1093/jee/toy133

Hebert PDN, Cywinska A, Ball SL, de Waard JR (2003) Biological identifications through DNA barcodes. Proceedings of the Royal Society Biological Sciences 270: 313–321. https://doi.org/10.1098/rspb.2002.2218

Heled J, Drummond AJ (2010) Bayesian inference of species trees from multilocus data. Molecular Biology and Evolution 27: 570–580. https://doi.org/10.1093/molbev/msp274

Hoang DT, Chernomor O, von Haeseler A, Minh BQ, Vinh LS (2018) UFBoot2: Imporving the ultrafast bootstrap approximation. Molecular Biology and Evolution 35: 518–522. https://doi.org/10.1093/molbev/msx281

Huang J, Wu J, An J, Williams PH (2015) Newly discovered colour-pattern polymorphism of *Bombus koreanus* females (Hymenoptera: Apidae) demonstrated by DNA barcoding. Apidologie 46: 250–261. https://doi.org/10.1007/s13592-014-0319-9

Hurtado-Burillo M, Jara L, May-Itzá WJ, Quezada-Euán JJG, Ruiz C, Rúa P (2016) A geometric morphometric and microsatellite analyses of *Scaptotrigona mexicana* and *S. pectoralis* (Apidae: Meliponini) sheds light on the biodiversity of Mesoamerican stingless bees. Journal of Insect Conservation 20: 753–763. https://doi.org/10.1007/s10841-016-9899-1

Kalyaanamoorthy S, Minh BQ, Wong TKF, von Haeseler A, Jermiin LS (2017) ModelFinder: Fast model selection for accurate phylogenetic estimates. Nature Methods 14: 587–589. https://doi.org/10.1038/nmeth.4285

Katoh K, Standley DM (2013) MAFFT multiple sequence alignment software version 7: improvements in performance and usability. Molecular Biology and Evolution 30: 772–780. https://doi.org/10.1093/molbev/mst010

Katoh K, Rozewicki J, Yamada KD (2019) MAFFT online service: multiple sequence alignment, interactive sequence choice and visualization. Briefings in Bionformatics 20: 1160–1166. https://doi.org/10.1093/bib/bbx108

Kim CK, Byrne LB (2006) Biodiversity loss and the taxonomic bottleneck: emerging biodiversity science. Ecological Research 21: 794–810. https://doi.org/10.1007/s11284-006-0035-7

Klingenberg CP (2011) MorphoJ: an integrated software package for geometric morphometrics. Molecular Ecology Resources 11: 353–357. https://doi.org/10.1111/j.1755-0998.2010.02924.x

Klingenberg CP (2015) Analyzing fluctuating asymmetry with geometric morphometrics: concepts, methods, and applications. Symmetry 7: 843–934. https://doi.org/10.3390/sym7020843

Kumar S, Stecher G, Li M, Knyaz C, Tamura K (2018) Mega X. Molecular evolutionary genetics analysis across computing platforms. Molecular Biology and Evolution 35: 1547–1549. https://doi.org/10.1093/molbev/msy096

Lachenbruch PA (1967) An almost unbiased method of obtaining confidence intervals for the probability of misclassification in discriminant analysis. Biometrics 23: 639–645. https://doi.org/10.2307/2528418

Lanfear R, Frandsen PB, Wright AM, Senfeld T, Calcott B (2017) PartitionFinder 2: new methods for selecting partitioned models of evolution for molecular and morphological phylogenetic analyses. Molecular Biology and Evolution 34: 772–773. https://doi.org/10.1093/molbev/msw2560

Lepeco A, Gonçalves RB (2018) The colour and the shape: Morphological variation on a facultatively eusocial bee *Augochlora* (*Augochlora*) *amphitrite* (Schrottky). Sociobiology 65: 662–670. https://doi.org/10.13102/sociobiology.v65i4.3388

Lepeletier de Saint Fargeau, A LM (1841) Histoire Naturelle des Insectes, Hyménoptères, Vol. 2. Librairie Encyclopédique de Roret, Paris, 680 pp.

López-Uribe MM, Zamudio KR, Cardoso CF, Danforth BN (2014) Climate, physiological tolerance and sex-biased dispersal shape genetic structure of Neotropical orchid bees. Molecular Ecology 23: 1874–1890. https://doi.org/10.1111/mec.12689

Machado C, Costa CP, Francoy TM (2018) Different physiognomies and the structure of Euglossini bee (Hymenoptera: Apidae) communities. Sociobiology 65: 471–481. https://doi.org/10.13102/sociobiology.v65i3.2718

Marques MF, Hautequestt AP, Oliveira UB, Manhães-Tavares VF, Perkles OR, Zappes CA, Gaglianone MC (2017) Local knowledge on native bees and their role as pollinators in agricultural communities. Journal of Insect Conservation 21: 345–356. https://doi.org/10.1007/s10841-017-9981-3

Martel C, Gerlach G, Ayasse M, Milet-Pinheiro P (2019) Pollination ecology of the Neotropical gesneriad *Gloxinia perennis*: chemical compostition and temporal fluctuation of floral perfume. Plant Biology 21: 723–731. https://doi.org/10.1111/plb.12974

Melo GAR (2014) Notes on the systematics of the orchid bee genus *Eulaema* (Hymenoptera: Apidae). Revista Brasileira de Entomologia 58: 235–240. https://doi.org/10.1590/S0085-56262014000300003

Michener CD (2007) The Bees of the World, 2nd Edn. Johns Hopkins University Press, Baltimore.

Moure JS (1960) Notes on the types of Neotropical bees described by Fabricius (Hymenoptera: Apoidea). Studia Entomologica 3: 97–160.

Moure JS (2000) As espécies do gênero *Eulaema* Lepeletier, 1841 (Hymenoptera, Apidae, Euglossinae). Acta Biologica Paranaense 29: 1–70. https://doi.org/10.5380/abpr.v29i0.582

Moure JS, Melo GAR (2022) Euglossini Latreille, 1802. In: Moure JS, Urban D, Melo GAR (Orgs) Catalogue of Bees (Hymenoptera, Apoidea) in the Neotropical Region - online version. http://www.moure.cria.org.br/catalogue [Accessed Aug/27/2022. Online since: 23 Jul 2008. Last update: 14 Apr 2022]

Nemésio A (2009) Orchid bees (Hymenoptera: Apidae) of the Brazilian Atlantic Forest. Zootaxa 2041: 1–242. https://doi.org/10.11646/zootaxa.2041.1.1

Nguyen LT, Schmidt HA, von Haeseler A, Minh BQ (2015) IQ-TREE: A fast and effective stochastic algorithm for estimating maximum likelihood phylogenies. Molecular Biology and Evolution 32: 268–274. https://doi.org/10.1093/molbev/msu300

Okonechnikov K, Golosova O, Fursov M (2012) Unipro UGENE: a unified bioinformatics toolkit. Bioinformatics 28: 1166–1167. https://doi.org/10.1093/bioinformatics/bts091

Oleksa A, Tofilski A (2014) Wing geometric morphometrics and microsatellite analysis provide similar discrimination of honey bee subspecies. Apidologie 46: 49–60. https://doi.org/10.1007/s13592-014-0300-7

Oliveira ML (2000) O gênero *Eulaema* Lepeletier, 1841 (Hymenoptera: Apidae: Euglossini): filogenia, biogeografia e relações com as Orchidaceae. PHD Thesis. Universidade de São Paulo (Brazil), 160 pp.

Oliveira ML (2006) Três novas espécies de abelhas da Amazônia pertencentes ao gênero *Eulaema* Lepeletier, 1841 (Hymenoptera: Apidae: Euglossini). Acta Amazonica 36: 273–286. https://doi.org/10.1590/S0044-59672006000100015

Packer L, Gibbs J, Sheffield C, Hanner R (2009) DNA barcoding and the mediocrity of morphology. Molecular Ecology Resources 9: 42–50. https://doi.org/10.1111/j.1755-0998.2009.02631.x

Padial JM, De La Riva I (2007) Integrative taxonomists should use and produce DNA barcodes. Zootaxa 1586: 67–68. https://doi.org/10.11646/ZOOTAXA.1586.1.7

Padial JM, Miralles A, De La Riva I, Vences M (2010) The integrative future of taxonomy. Frontiers in Zoology 7: 16. https://doi.org/10.1186/1742-9994-7-16

Pires EP, Morgado LN, Souza B, Carvalho CF, Nemésio A (2013) Community of orchid bees (Hymenoptera: Apidae) in transitional vegetation between Cerrado and Atlantic Forest in southeastern Brazil. Brazilian Journal of Biology 73: 507–513. https://doi.org/10.1590/S1519-69842013000300007

Pokorny T, Lunau K, Quezada-Euán JJG, Eltz T (2014) Cuticular hydrocarbons distinguish cryptic sibling species in *Euglossa* orchid bees. Apidologie 45: 276–283. https://doi.org/10.1007/s13592-013-0250-5

Quezada-Euán JJG, Sheets HD, de Luna E, Eltz T (2015) Identification of cryptic species and morphotypes in male *Euglossa*: Morphometric analysis of forewings (Hymenoptera: Euglossini). Apidologie 46: 787–795. https://doi.org/10.1007/s13592-015-0369-7

Rambaut A (2018) Figtree: tree figure drawing tool version 1.4.4. http://tree.bio.ed.ac.uk/software/figtree

Rambaut A, Drummond AJ, Xie D, Baele G, Suchard MA (2018) Posterior summarization in Bayesian phylogenetics using Tracer 1.7. Systematic Biology 67(5): 901–904. https://doi.org/10.1093/sysbio/syy032

Rocha-Filho LC, Garófalo CA (2015) Males of the orchid bee *Eulaema cingulata* (Hymenoptera: Apidae) as important vectors of the cleptoparasitic beetle *Meloetyphlus fuscatus* (Coleoptera: Meloidae). Apidologie 46: 286–291. https://doi.org/10.1007/s13592-014-0322-1

Rocha-Filho LC, Cerântola NCM, Garófalo CA, Imperatriz-Fonseca VL, Del Lama MA (2013) Genetic differentiation of the Euglossini (Hymenoptera, Apidae) populations on a mainland coastal plain and an island in southeastern Brazil. Genetica 141: 65–74. https://doi.org/10.1007/s10709-013-9706-9

Rohland N, Reich D (2012) Cost-effective, high-throughput DNA sequencing libraries for multiplexed target capture. Genome Resources 22: 939–946. https://doi.org/10.1101/gr.128124.111

Rohlf FJ (2006) TpsDig, 2.0. Department of Ecology and Evolution, State Univ. of New York at Stony Brook, Stony Brook, NY.

Rohlf FJ (2013) TpsUtil. Department of Ecology and Evolution, State University of New York, Stony Brook, NY, USA. http://life.bio.sunysb.edu/morph/

Ronquist F, Teslenko M, Mark PVD, Ayres DL, Darling A, Höhna S, Larget B, Liu L, Suchard MA, Huelsenbeck J (2012) MrBayes 3.2: Efficient Bayesian phylogenetic inference and model choice across a large model space. Systematic Biology 61: 539–542. https://doi.org/10.1093/sysbio/sys029

Rubinoff D, Cameron S, Will K (2006) A genomic perspective on the shortcomings of mitochondrial DNA for "barcoding" identification. Journal of Heredity 97: 581–594. https://doi.org/10.1093/jhered/esl036

Schlick-Steiner BC, Steiner FM, Seifert B, Stauffer C, Christian E, Crozier RH (2010) Integrative taxonomy: a multisource approach to exploring biodiversity. Annual Review of Entomology 55: 421–438. https://doi.org/10.1146/annurev-ento-112408-085432

Silva FL, Grassi-Sella ML, Francoy TM, Costa AHR (2015) Evaluating classification and feature selection techniques for honeybee subspecies identification using wing images. Computers and Electronics in Agriculture 114: 68–77. https://doi.org/10.1016/j.compag.2015.03.012

Silveira GC, Freitas RF, Tosta THA, Rabelo LC, Gaglianone MC, Augusto SC (2015) The orchid bee fauna in the Brazilian savanna: do forest formations contribute to higher species diversity? Apidologie 46: 197–208. https://doi.org/10.1007/s13592-014-0314-1

Smith BT, Harvey MG, Faircloth BC, Glenn TC, Brumfield RT (2013) Target capture and massively parallel sequencing of ultraconserved elements (UCEs) for comparative studies at shallow evolutionary time scales. Systematic Biology 63: 83–95. https://doi.org/10.1093/sysbio/syt061

Souza DA, Wang Y, Kaftanoglu O, De Jong D, Amdam GV, Gonçalves LS, Francoy TM (2015) Morphometric identification of queens, workers and intermediates in *In Vitro* reared honey bees (*Apis mellifera*). PLoS ONE 10: e0123663. https://doi.org/10.1371/jounal.pone.0123663

Sukumaran J, Knowles LL (2017) Multispecies coalescent delimits structure, not species. Proceedings of the National Academy of Sciences 114: 1607–1612. https://doi.org/10.1073/pnas.1607921114

Tagliacollo VA, Lanfear R (2018) Estimating improved partitioning schemes for ultraconserved elements. Molecular Biology and Evolution 35: 1798–1811. https://doi.org/10.1093/molbev/msy069

Watteyn C, Scaccabarozzi D, Muys B, Meerbeek K, Ackerman JD, Fonseca MVC, Alvarado IFC, Reubens B, Huarcaya RP, Cozzolino S, Karremans AP (2021) Trick or treat? Pollinator attraction in *Vanilla pompona* (Orchidaceae). Biotropica 54: 268–274. https://doi.org/10.1111/btp.13034

Wheeler QD (2008) Undisciplined thinking: morphology and Hennig's unfinished revolution. Systematic Entomology 33: 2–7. https://doi.org/10.1111./j.1365-3113.2007.00411.x

Zhang C, Rabiee M, Sayyari E, Mirarab S (2018) ASTRAL-III: polynomial time species tree reconstruction from partially resoled gene trees. BMC Bioinformatics 19: 153. https://doi.org/10.1186/s12859-018-2129-y

Supplementary material 1

Integrative taxonomy of *Eulaema cingulata*

Authors: Tamires de Oliveira Andrade, Kelli dos Santos Ramos, Margarita M. López-Uribe, Michael G. Branstetter, Carlos Roberto F. Brandão

Data type: tables (ms word file)

Explanation note: tables: Voucher ID, locality data, and institutional repositories of the male specimens of *Eulaema* used in Geometric Morphometric analyses; Voucher ID, locality data, and institutional repositories of the specimens used both in COI and phylogenomic analyses; Results of the Principal Component Analysis (PCA) of head analysis with their respective percentage of variance; Results of the Principal Component Analysis (PCA) of wing analysis with their respective percentage of variance.

Link: https://doi.org/10.3897/jhr.94.91001.suppl1